

# ESTIMATION OF LATENT HEAT FLUX OVER OCEANS

W. Timothy Liu  
Jet Propulsion Laboratory  
California Institute of Technology  
Pasadena, California, U.S.A.

## 1. INTRODUCTION

Evaporation is the principal mechanism to transport water from the surface of the Earth to the atmosphere and the ocean covers over 70% of the Earth's surface. With its high specific heat and large thermal inertia, the ocean is a large reservoir of heat and the flywheel of the global heat engine. Since water has high latent heat, evaporation is also an efficient way to redistribute energy and change climate.

Like momentum and sensible heat, water vapor and latent heat are transported from the ocean to the atmosphere mainly by turbulence. The measurement of these turbulent transports will be discussed in Section 2. The measurement of the microscale turbulent flux requires sophisticated instrumentation and the bulk parameterization method is used to relate the flux to a few more readily-available parameters averaged over certain time periods and grid sized. This method is discussed in Section 3. In the past, the measurement of the bulk parameters are provided by routine meteorological reports from volunteer ships which are not adequate to resolve the needed temporal and spatial variabilities. Spaceborne sensors can provide repeated and uniform observations. Methods of estimating latent heat flux from satellite data are discussed in Section 4. A few applications of the flux from satellite data are discussed in Section 5. Atmospheric general circulation models (AGCM), such as the one at the European Centre for Medium Range Weather Forecast (ECMWF), have the potential of providing useful dynamic interpolation of sparse measurements in time and space. A comparison of ECMWF latent heat flux with satellite products will be given in Section 6. Section 7 is the conclusion.

## 2. MEASURING TURBULENT FLUXES

The most direct method of measuring evaporation is the eddy correlation method which makes use of the definition,  $E = \rho \langle Q'U_3' \rangle$ , where  $E$  is the water vapor flux,  $\rho$  is the surface air density,  $Q$  is the specific humidity,  $U_3$  is the vertical component of wind, the bracket indicates time average and the primed quantities are the deviations from the average. The product of  $E$  and the latent heat of vaporization is the latent heat flux. Since this method requires the vertical component of wind, a rigid slender supporting structure is needed, so that  $U_3'$  would not be contaminated by the motion of the support and flow distortion. This requirement generally excludes conventional ships and buoys as platforms and most of such measurement were made on research towers or specially designed ships (e.g., Pond et al., 1971). This method, however, has been used on aircraft with good inertial systems to correct for plane motion (e.g., Nicholls and Reading, 1979).

The dissipation method is based on the assumption of the balance between turbulence production term and dissipation term in the equation of the conservation of moisture variance (Busch, 1977); the non-stationary term and the divergence term are assumed to be negligibly small. Since the production term is defined in terms of the fluxes, we can derive the fluxes with the measurement of dissipation. In the so called inertial subrange of frequencies, the spectral density follows a  $-5/3$  power law with frequencies, and it can be related to the

dissipation rate through Kolmogoroff hypothesis. The appeal of this method is that it can be done on ship; the vertical component of wind is not required and the inertial subrange occurs at higher frequencies than ship motions. The dissipation method involved a few assumptions and constants that are not well established. However, good agreement between fluxes obtained by the dissipation method and by the eddy correlation methods have been demonstrated by Large and Pond (1982) in North Atlantic and by Edson et al. (1988) in the North Sea, with wind speed ranging approximately from 5 to 22 m/s. The validity of the dissipation method under low wind condition remains to be demonstrated. Under light winds, the problem of ship motion on the correlation method is much less severe. Bradley et al. (1990) measured the moisture flux by both methods in the doldrum of the Western tropical Pacific and found that the dissipation method underestimates the flux under light winds.

Before the advent in computer to handle the large amount data processing required for the correlation or dissipation methods, computation of the flux depends on the gradient (or profile) method. Under neutral stability, atmospheric wind, temperature and humidity scaled by the fluxes vary logarithmically with height (see discussion in Section 2). By measuring mean wind, temperature and humidity at several levels and plot them against the logarithmic height, the fluxes of momentum, sensible and moisture can be derived from the slope of the linear regression. If the atmosphere is not near neutral, the relation will deviate from linear and graphical methods or numerical iterations have to be used. Since the gradient over ocean is small, the profile method demands high sensor precision. If we use different instrument at different height, the difference in instrument errors may be bigger than the real signal. If we move the same sensor up and down, there will be a time difference and the movement may disturbs the atmosphere (e.g., Paulson et al., 1972).

## 2. BULK PARAMETERIZATION

The methods discussed in Section 1 have high demand on instrumentation and have been used only for a limited period of time at selected locations. For long period and large scale fluxes, the only practical method is the bulk parameterization formula,

$$E = \rho C_E U (Q_s - Q) \quad (1a)$$

To the first approximation, E is assumed to be proportional to the product of wind speed (U) and the sea-air specific humidity difference ( $\Delta Q = Q_s - Q$ ). The specific humidity at the sea-air interface ( $Q_s$ ) is assumed to be the saturation humidity at sea surface temperature ( $T_s$ ). The proportionality constant ( $C_E$ ), called the transfer coefficient, is usually determined from the slope of the linear regression between E and  $U\Delta Q$  measured during field experiments. There is usually a large scatter of the data above such linear regression. In theory,  $C_E$  depends on the height at which U and Q are measured and also on conditions such as the roughness of the sea and the density stratification of the atmosphere. A bulk formula with a constant transfer coefficient is a simple but useful tool if one could tolerate the inaccuracy. In the past, the coefficients were determined and verified with data under moderate wind conditions, approximately between 4 to 15 m/s. Using direct measurement of E from a number of experiments, Friehe and Schmitt (1976) found  $C_E$  to be  $1.3 \times 10^{-3}$ . Large and Pond (1982) measured the flux by the dissipation method, and found a value of  $1.15 \times 10^{-3}$ . The extrapolation of the empirical values to high and low winds were controversial. At low winds, the sea surface changes from rough to smooth with different transfer processes. At high winds, breaking waves and sprays provide different mechanisms of introducing water sources into the atmosphere. Most of the recent field experiments are directed at these extreme conditions. The equations for sensible heat flux H,

$$H = \rho c C_H U (T_s - T) \quad (1b)$$

and wind stress  $\tau$  (momentum flux),

$$\tau = \rho C_D U^2 \quad (1c)$$

are similar, where  $c$  is the isobaric specific heat,  $U$  and  $T$  are the wind speed and temperature in the atmospheric surface layer,  $C_H$  is the transfer coefficient for sensible heat and  $C_D$  is the transfer coefficient for momentum (also called the drag coefficient).

Liu et al. (1979) tried to account for the variabilities of  $C_E$  by solving simultaneously three equations representing the three similarity profiles of wind, temperature and humidity (1) for the three unknowns  $E, H, \tau$ . The similarity relations are

$$(Q - Q_s)/Q_* = 2.2 \ln(z/z_Q - \psi_Q) = C_D^{1/2} C_E^{-1}. \quad (2a)$$

$$(T - T_s)/T_* = 2.2 \ln(z/z_T - \psi_T) = C_D^{1/2} C_H^{-1}, \quad (2b)$$

$$(U - U_s)/U_* = 2.5 \ln(z/z_0 - \psi_U) = C_D^{-1/2}, \quad (2c)$$

By definition,  $U_*, T_*, Q_*$  are function of  $\tau, H,$  and  $E$ . The  $\psi_U, \psi_T,$  and  $\psi_Q$  are function of the stability parameter and can be expressed in terms of the three fluxes. The lower boundary parameters  $z_0, z_T,$  and  $z_Q$  are functions of  $\tau$  and fluid properties. The surface speed  $U_s$  is generally assumed to be zero. This method is equivalent to using transfer coefficients which vary with height and the bulk parameters.

Under neutral stability ( $\psi_U = \psi_T = \psi_Q = 0$ ), the variabilities of the coefficients are governed by the variabilities of  $z_0, z_T,$  and  $z_Q$ . The three parameters reflect the transport processes near the surface as illustrate in Fig. 1, which includes the velocity and temperature distributions measured in smooth channels by Reichardt (1940) and Deissler & Eian (1952). Away from the surface, the flow is turbulent and the measurements follow a logarithmic law. Near the surface, viscosity and conductivity become important and the profiles agree with the postulation based on a model by Liu et al. (1979). The imagery height at which the  $U - U_s = 0$  along the extrapolation of the logarithmic profile is  $z_0$ . The interpretation of  $z_T$  and  $z_Q$  are the same except for temperature and specific humidity. Schlichting (1968) suggested that a surface is aerodynamically rough when the roughness elements penetrate the viscous sublayer and it is smooth if the sublayer covers the roughness elements. The scaling depth of the sublayer is  $\nu/U_*$ , where  $\nu$  is the kinematic viscosity. Alternatively, rough flow can be viewed as the state when the local velocity scale and the characteristic scale of the roughness elements,  $\xi$ , combined to form a roughness Reynolds Number ( $\xi U_*/\nu$ ) that exceed a critical value. The velocity measurements in pipe flow by Nikuradse (1933) are shown in Fig. 2.  $\xi$  is the actual mean diameter of the sand-grains used as roughness elements. The measurements of Kondo (1975) at an air-sea interface are shown in Fig. 2 and  $\xi$  is the square root of the integral of the one dimensional wave spectrum between two selected frequencies. In smooth flow,  $\xi \ll \nu/U_*$ , momentum is mainly transported by viscosity,  $z_0$  is proportional to  $\nu/U_*$ , and, therefore,  $C_D$  increases with decreasing  $U_*$ . When the interface is smooth, Liu et al. (1979) postulated that momentum, heat and water vapor are all transported by molecular processes near the interface and the variations of  $C_D, C_H,$  and  $C_E$  should share the same characteristics, i.e., increases with decreasing winds. Fig. 3 shows the values of  $C_E$  given by the model of Liu et al (1979) as a function of  $U$  and  $\Delta Q$ , assuming a reference height of 10 m, a  $T_s$  of 25°C, and a relative humidity of 80%. The values at low winds were recently confirmed by the field measurements of Bradley et al. (1990). Such behavior is necessary to provide for buoyancy-induced turbulent transport as the mean wind vanishes. Palmer et al. (1990) found it critical to include such behavior in the operational model of ECMWF to realistically simulate observed monsoon circulation and associated rainfall.

In rough flow,  $\xi \gg \nu/U_*$ , momentum is mainly transported by pressure force on the roughness element and the flow is independent of  $\nu$ , and  $z_0$  is proportional to  $\xi$ . In the case of a rough sea surface,  $\xi$  increases with wind and, therefore,  $C_D$  increases with wind. Charnock (1955) postulated that  $z_0$  is proportional to  $U_*^2/g$  where  $g$  is the acceleration due to gravity. When the

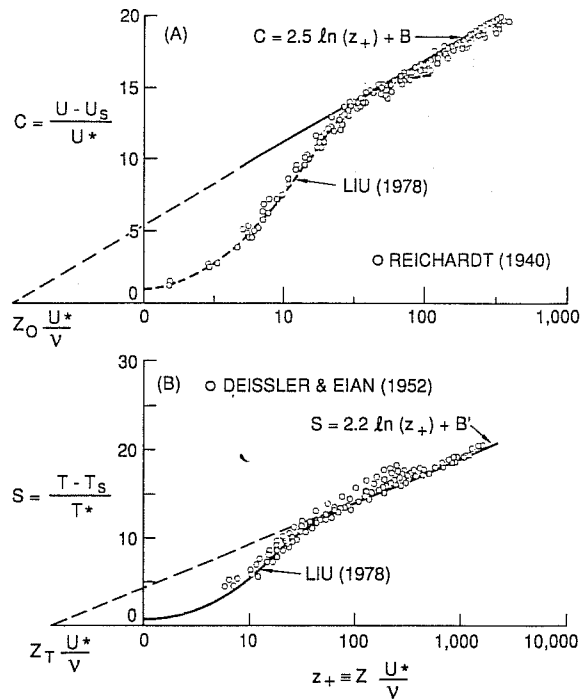


Fig.1 Laboratory measurements of the vertical profiles of (A) velocity and (B) temperature, (from Liu et al. 1979).

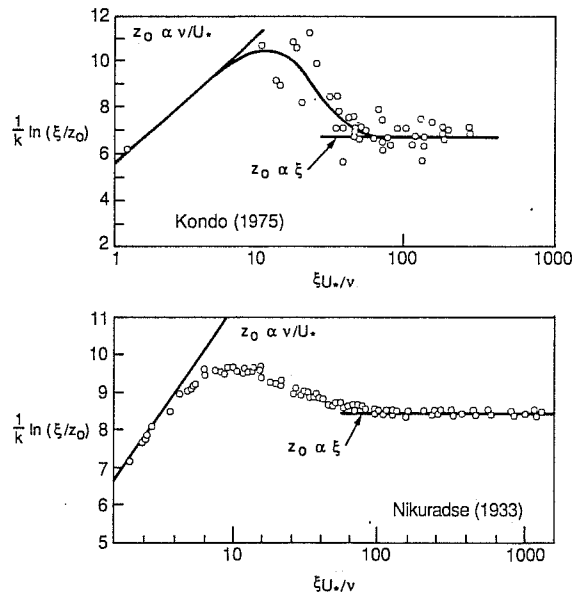


Fig.2 Variation of the roughness parameter at the sea-air interface (top), and in pipe flow (bottom), (from Liu et al., 1979).

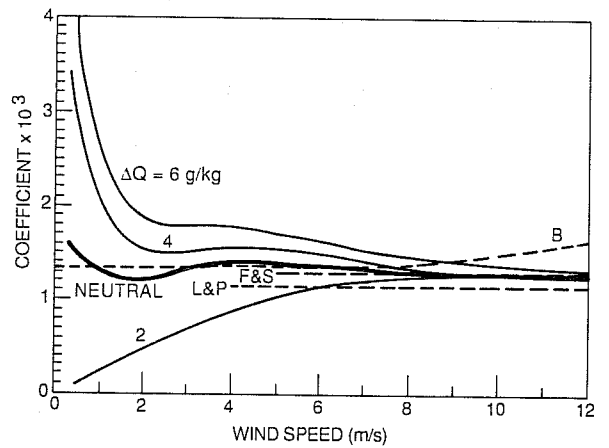


Fig.3 Variation of the moisture coefficient with wind and sea-air humidity difference computed with model of Liu et al. (1979).

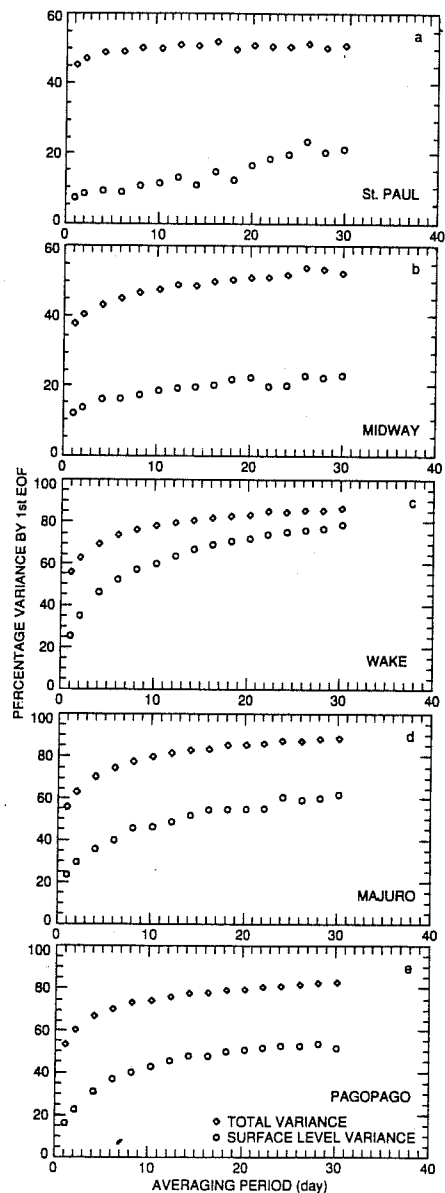


Fig.4 Percentage variance of specific humidity represented by the first EOF at various averaging periods

roughness of the surface increases, turbulent transport is facilitated, and  $C_D$  increases with wind speed. While momentum can be transported by pressure forces on the roughness elements independent of viscosity, the slow molecular diffusion is the only process which transport heat and mass at the interface. Increase in roughness increases the sheltering effect, and the fluid stays longer in contact with the surface before turbulence carries it away. The opposing effects on the  $C_E$ , as postulated by Liu et al. (1979), can be seen in Fig. 3. Under near neutral stability, Liu et al. (1979) gave  $C_E$  a value of approximately  $1.3 \times 10^{-3}$  at moderate winds and the value decreases a little with increasing winds. This agrees approximately with the results of Friehe and Schmitt (1978) and Large and Pond (1982). At high winds, preliminary results from an experiment in the North Sea pointed to a constant value of  $1.2 \times 10^{-3}$  (Smith and Anderson, 1988). The value of Bunker (1976), however, increases with wind speed, following the characteristics of  $C_D$ . An updated version of Liu et al. (1979) with smooth transition between smooth and rough flow ( $2\text{m/s} < U < 5\text{m/s}$ ) is being developed. The coefficient also depends on atmospheric stability governed by the density stratification. Over the warm water of tropical ocean, Liu (1988) demonstrated that the humidity is as important as temperature in producing buoyancy and destabilizing the atmosphere and  $C_E$  is clearly dependent on  $\Delta Q$  as shown in Fig. 3.

Although Bradley et al. (1990) indicated that the model of Liu et al. (1979) match their observations down to wind speeds of 0.5 m/s, the similarity profiles are not valid under free convection when buoyancy completely dominates over wind shear in turbulence production. In open oceans, free convection is rare and is not well studied. However, there are many studies of free convection of homogeneous fluids, particularly in laboratory. Liu (1984) gave a detailed review. Krishnamurti (1973) showed that the circulation in a fluid goes from laminar to fully turbulent as the Raleigh number for temperature ( $Ra_T \equiv \alpha g \Delta T d^3 / (\kappa_T \nu)$ ) increases. In the definition of  $Ra_T$ ,  $\alpha$  is the coefficient of thermal expansion and  $\kappa_T$  is the thermal conductivity. When the flow is fully turbulent, theoretical and empirical studies suggest that the heat transport is governed by

$$Nu = A Ra_T^{1/3} \quad (4)$$

where  $Nu \equiv Hd / (\rho c \kappa_T \Delta T)$  is the Nusselt number, and  $A$  depends on the Prandtl Number  $Pr = \nu / \kappa_T$ . This relation was confirmed by a laboratory measurement in an open tank of water with no mean winds (Liu 1974; Katsaros et al. 1977). This relation can be reduced to

$$H = A \rho c \left( \frac{\alpha g \kappa_T^2}{\nu} \right)^{1/3} \Delta T^{4/3} \quad (5)$$

The relation between  $Q$  and  $\Delta T$  is independent of the depth of fluid. For a inhomogeneous fluid like the atmosphere over ocean, (4) can be generalized to include moisture transport,

$$Nu = A \left[ Ra_T + Ra_Q \left( \frac{Pr}{Sc} \right)^{3/2} \right]^{1/3} \quad (6a)$$

$$Sh = A \left[ Ra_Q + Ra_T \left( \frac{Sc}{Pr} \right)^{3/2} \right]^{1/3} \quad (6b)$$

where  $Sh \equiv Ed / (\rho \kappa_Q \Delta Q)$  is the Sherwood number,  $Sc = \nu / \kappa_Q$  is the Schmidt number,  $\kappa_Q$  is the diffusivity of water vapor,  $Ra_Q = \beta g \Delta Q d^3 / \kappa_Q \nu$  is the Raleigh number for humidity, and  $\beta$  is the expansion coefficient due to water vapor. The heat and moisture fluxes can be reduced to functions of  $\Delta T$  and  $\Delta Q$ . Golitsyn and Garchov (1986) have tested these relations with measurements.

Wyngaard et al. (1971) recognized that the similarity theory breaks down at zero  $U$ , and introduced a free convection scale for an atmospheric mixed layer with a depth  $d$ ,

$$U_f = \left( \frac{\alpha g d H}{c_p} \right)^{1/3} \quad (7)$$

and Businger (1973) postulated that convection will induce local surface friction velocity,  $U^*$  and  $U^*/U_f$  is a decreasing function of  $d/z_0$ . Assuming

$$\frac{U^*}{U_f} \propto \left( \frac{d}{z_0} \right)^{-1/3} \quad (8)$$

and that the resident time scale of the fluid at the surface is equal to the Kolmogorov time scale, Liu et al. (1979) derived (4) from (8). Schuman (1988) suggested that (4) is applicable only to smooth flow. In rough flow, he suggested

$$Nu = A Ra_T^{1/2} \quad (9)$$

Under free convection conditions, the flow is always smooth over the ocean. The independence of heat flux from any depth scale, as in (6), remains to be vigorously tested. The  $H$  and  $E$  given by Liu et al. (1979) approach those given by (6) asymptotically as the mean wind vanishes. There are different ways of formulating such transition, essentially by eliminating the dependence on  $z$  and  $U^*$  in (2a) and (2b). Vigorous examinations of these approaches are underway.

### 3. SATELLITE DATA

In the past,  $U$ ,  $T_s$  and  $Q$  measurements are provided by routine meteorological reports from volunteer ships. Except near coastal areas and in major shipping lanes, these reports are sparse and not adequate to resolve the needed temporal and spatial variabilities. Spaceborne sensors would provide repeated and uniform coverage. At present, spaceborne sensors can measure  $U$  and  $T_s$  but not  $Q$ . Microwave radiometers, however, can measure accurately the column-integrated water vapor in the atmosphere ( $W$ ). A global relation between monthly mean  $Q$  and  $W$  was derived using 17 years of radiosonde reports from 46 mid-ocean meteorological stations (Liu, 1986). The  $Q$  derived from  $W$  measured by the microwave radiometer on Nimbus-7 was used with surface wind speed and sea surface temperature to compute the evaporation and latent heat flux in the tropical Pacific (Liu, 1988).

The application of satellite data to compute  $E$  was confined to monthly means. Hsu and Blanchard (1989) evaluated the  $Q$ - $W$  relation by Liu (1986) with measurements taken in 13 field experiments distributed over global oceans and indicated that the relation could be used to describe not only monthly mean, but also instantaneous soundings. The relation has been applied to derived daily evaporation by a number of investigators with various degree of success. The validity of the  $Q$ - $W$  relation at periods shorter than a month depends on how well the relation accounts for the high frequency variability of atmospheric humidity. Using empirical orthogonal function analysis, Liu et al. (1991) demonstrated that, in the tropical oceans for example, such single-parameter estimation can account for, at most, 60% of the daily variance but it can represent up to 90% of the variance for periods longer than 10 days. Fig.4 shows the total percentage variance and the percentage variance at the surface represented by the first EOF as a function of averaging period. The five stations stretch from the Arctic to the Southern Pacific. At each location, there is an inflection point at approximately 10 days. The amount of variance represented by one independent mode decreases rapidly below seven days. With periods longer than 14 days, the amount of variance represented by the first EOF does not change much and a single mode of variability dominates. Methods to increase the accuracy of  $Q$  estimation at high frequencies were discussed by Liu et al. (1991).

#### 4. APPLICATION OF LATENT HEAT FLUX FROM SATELLITE DATA

Liu (1988) derived approximately four years of latent heat flux in the tropical Pacific using data from the microwave radiometer (SMMR) of Nimbus-7. The period includes one an El Niño Southern Oscillation (ENSO) episode, a major climate anomaly in the area. Despite the anomalously high sea surface temperature, evaporation was found to be anomalously low in the equatorial Pacific during the early phase of the ENSO episode in 1982 because of the low wind speed resulted from surface convergence associated with deep convection. The normal maximum mean sea surface temperature is located in the broad area across the equator in the west and a zonal band just north of the equator in the east. However, relatively low evaporation was found in these areas due to the low mean wind speed. The high precipitable water in the colocated deep convections are fed by surface advection.

Liu and Gautier (1990) combined these latent heat flux fields with the shortwave radiation derived from GOES observations to approximate the surface thermal forcing. Ocean's response was expressed as the time rate of change of sea surface temperature. Starting from February 1980, 46 months of data were used to determine the correlation coefficient between the forcing and the response at each  $2^\circ$  latitude by  $2^\circ$  longitude area (Fig. 5A). Away from the equator, the correlations are significant, indicating that the seasonal change of sea surface temperature is dominated by surface thermal forcing. In the equatorial wave guide ( $5^\circ$  N to  $5^\circ$  S), there is almost no correlation, and ocean dynamic appears to be more important than surface flux in governing the sea surface temperature change. Away from the equator, the seasonal variations of the forcing and response are found to be in phase, high in the summer and low in the winter. With the seasonal cycle removed from 22 month of data, starting January 1982, the time series of deviations (anomalies) formed were used to compute correlations (Fig. 5B). The distribution of correlation coefficients between anomalous latent heat flux and anomalous time rate of change of sea surface temperature shows positive significant values in the equatorial and southern ocean, in an area which was approximately occupied by the most intense sea surface temperature anomalies during the episode. Surface latent heat flux appears to play a more important role in the anomalous change than expected.

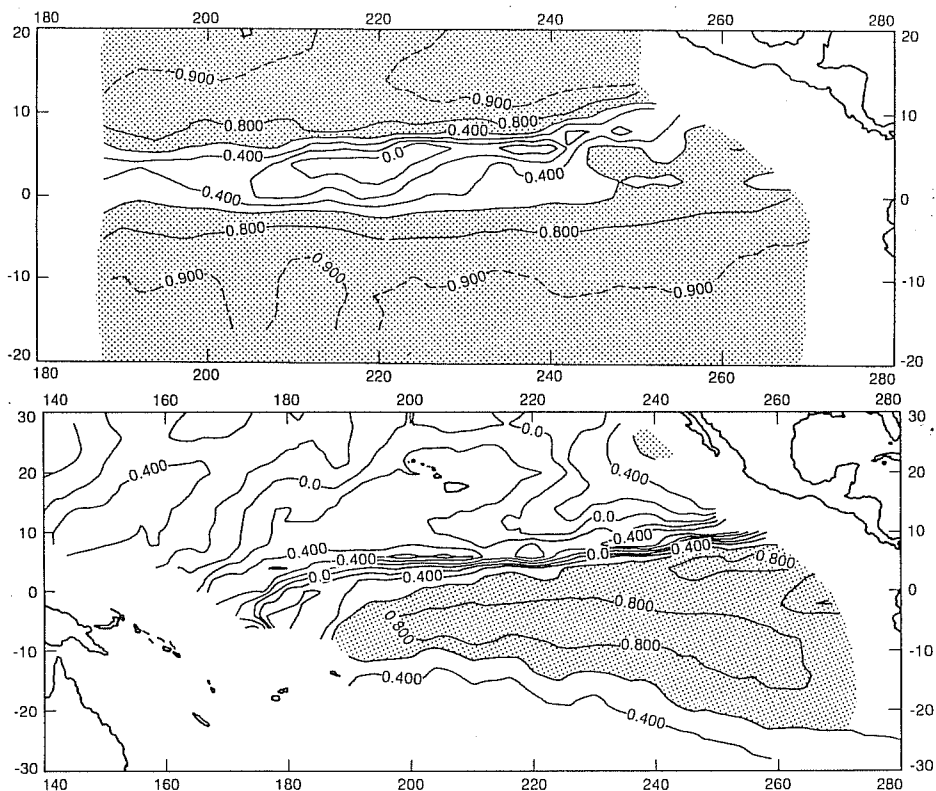


Fig. 5. Distribution of correlation coefficients (upper) between surface net heat flux and time rate of change of sea surface temperature and (lower) between the anomalies of latent heat flux and the anomalies of the time rate of change of sea surface temperature.

The high correlation between forcing and response outside the equatorial wave-guide may support one-dimensional mixed layer models. The combined thermal and wind forcing in the tropical Pacific was expressed as a Monin-Obuhkov length  $L = aU_*^3/F$ , where  $a$  is assumed to be a constant and  $F$  is the sum of latent heat and shortwave radiation. The frictional velocity  $U_*$  was derived from the wind speed measured by SMMR and  $F$  was computed using satellite data as described above. The mixed layer depth is defined as the depth at which temperature is  $1^\circ\text{C}$  lower than surface value in the climatological temperature soundings compiled by Levitus. A preliminary comparison (Fig. 6) shows that the seasonal changes of  $L$  agree approximately with the change in mixed layer depth at both  $16^\circ\text{N}$  and  $16^\circ\text{S}$ . At  $16^\circ\text{N}$ , highest values are found in winter-spring and lowest values in summer-autumn and the values decrease from west to east. At  $16^\circ\text{S}$ , the maxima is in winter and minima in summer, with a slight phase shift in the east and the depths are rather uniform in zonal distribution.

#### 4. COMPARISON WITH AGCM PRODUCTS

One of the products of the ECMWF AGCM is surface latent heat flux. Simonot and Le Treut (1987) examine the monthly mean evaporation from 1983 to 1985 and found that the values are systematically biased low by approximately  $40 \text{ W/m}^2$ . Liu (1988) examined the 1983 products and indicated that they were not adequate to capture the zonal gradient and interannual variability in the tropical Pacific. In 1985, the AGCM of ECMWF received several important improvement, including shallow convection that enhance evaporation.

The Special Sensor Microwave Imager (SSM/I) was launched in 1987 on the operational spacecraft of the Defense Meteorological Space Program. Starting July 1987, latent heat flux fields over global oceans were computed with the model of Liu et al. (1979), using  $U$  and  $W$  from SSM/I and the  $T_s$  from the Advanced Very High Resolution Radiometer. It appears worthwhile to compare the new model results with new satellite products. The transfer coefficient used in the AGCM of ECMWF is different from Liu et al. (1979). To eliminate the difference caused by the use of different coefficients as discussed in Section 2, latent heat flux fields were also computed with the model of Liu et al. (1979) for the same period, using the  $U$ ,  $T_s$  and  $Q$  fields in the Basic Level III Data Sets in the ECMWF/WCRP Level III-A Global Atmospheric Data Archive. The flux using ECMWF parameters are found to be significantly lower than those computed from satellite data in the eastern part of the tropical oceans in the Southern Hemisphere (Fig.7). The cause is found mainly to be overestimation of  $Q$  by the AGCM in these areas.

Fields of  $Q$  over global oceans were first derived from  $W$  measured by SSM/I, and fields of  $Q$  from ECMWF were then subtracted. The distribution of the difference in October 1987 is shown in Fig. 8A as an example. The  $Q$  from SSM/I is lower than  $Q$  from AGCM by  $4 \text{ g/Kg}$  in four areas (hatched in Fig. 9a); off the coast of Peru, Namibia, Saudi Arabia, and west coast of Australia. These are the same area where we found large flux differences. To make sure that the difference is not introduced by the relation of Liu (1986), the difference between  $W$

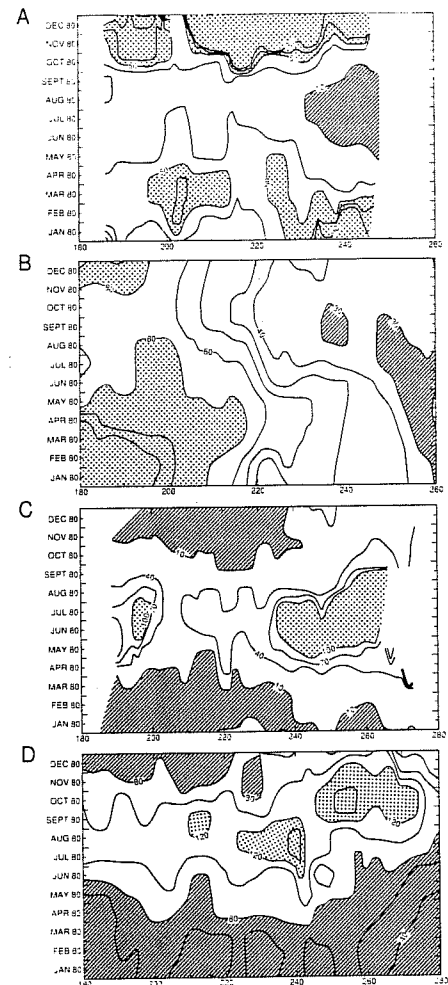


Fig. 6. Time-longitude variations in the Pacific (from top to bottom) Monin Obuhkov depth at  $16^\circ\text{N}$ , mixed layer depth at  $16^\circ\text{N}$ , Monin Obuhkov depth at  $16^\circ\text{S}$ , and mixed layer depth at  $16^\circ\text{S}$ .



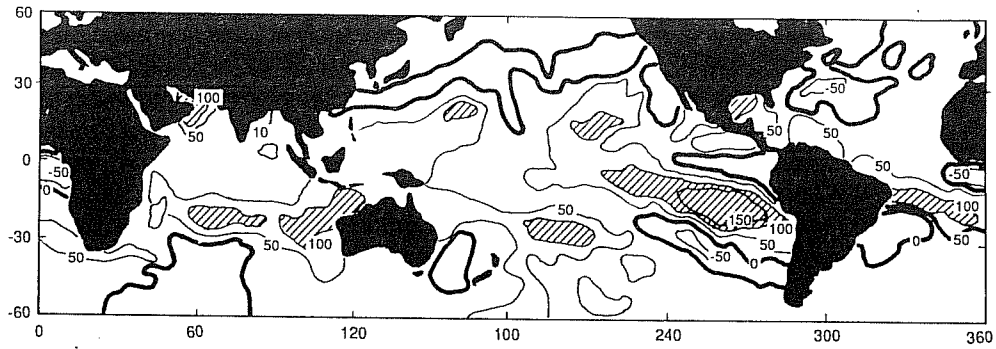


Fig 7 Distribution of the difference between latent heat flux derived from SSMI observations and derived from ECMWF paramters. Isolines are in  $W/m^2$

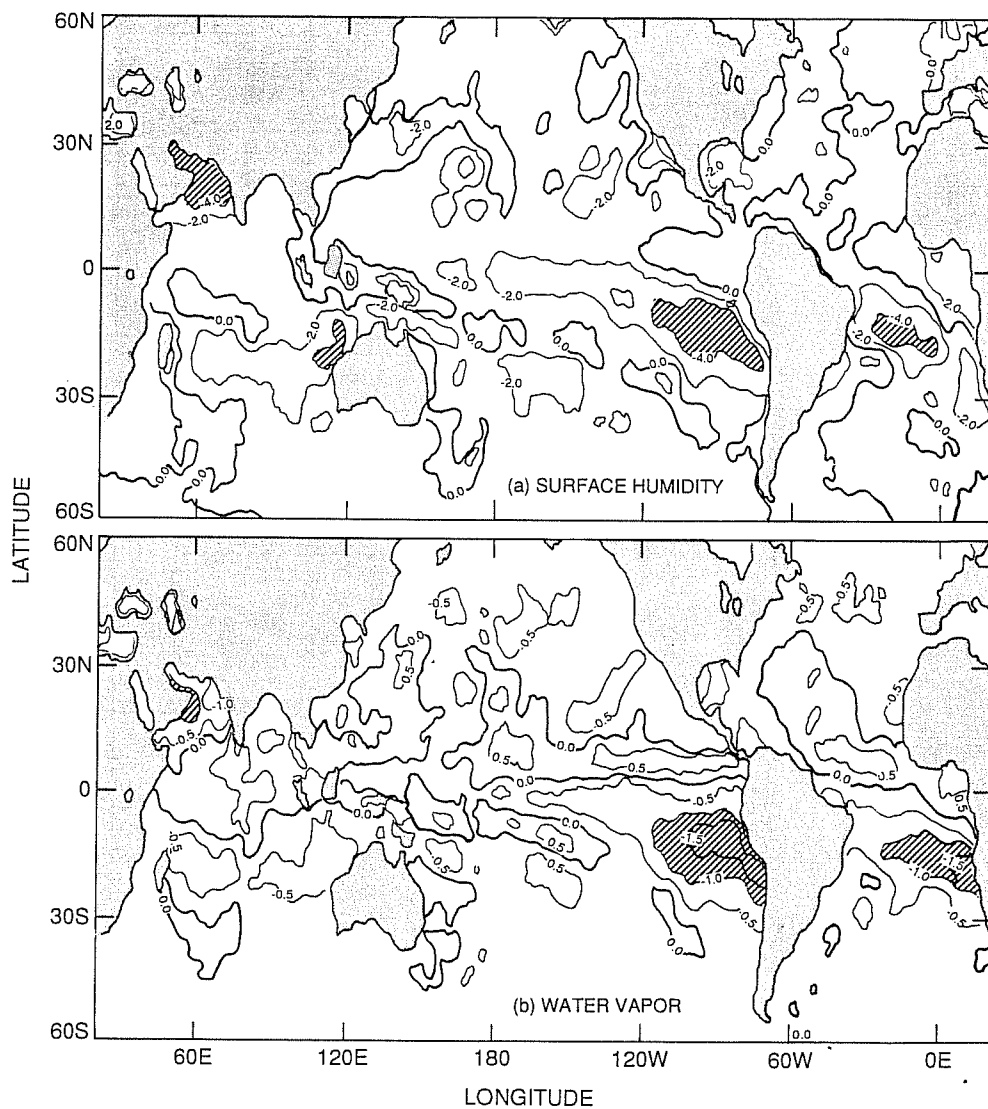


Fig. 8 Distributions of (A) the difference between surface level specific humidity derived from SSMI observations produced by the general circulation model of ECMWF (b) the difference between integrated water vapor in the atmospheric column derived from SSMI observations and derived from ECMWF model products.

W measured by SSMI and W obtained by integrating the humidity at all atmospheric levels produced by AGCM is show in Fig. 8B. The distribution is very similar to those of Q difference; the same areas of significant difference are found. The W data from SSMI used in Fig. 8 are derived using the algorithm by Wentz et al. (1983). Similar distributions are found using two other algorithms (Schlüssel and Emery, 1990; Alishouse et al., 1990).

Radiosonde reports will show if the satellite measurements or the AGCM products are in error. However, radiosonde in these areas are scarce. Comparisons with radiosonde data from July 1987 to December 1988 at three locations are shown in Fig. 9 as examples. The W climatology derived from Geophysical Fluid Dynamic Laboratory Atmospheric Statistics (Oort, 1983) are also shown. St Helena (16°S, 6°W) is located in eastern South Atlantic, Muscat (24°N, 58°E) at the tip the Arabian Peninsular adjacent to the Gulf of Oman, and Cape Verde (17°N, 23°W) in the eastern North Atlantic. During this period, St. Helena has 16 months of radiosonde data, but Muscat and Cape Verde have only 6. At all three locations, ECMWF data are higher than satellite data through the year, with largest difference during summer. The radiosonde data are obviously in closer agreement with satellite data.

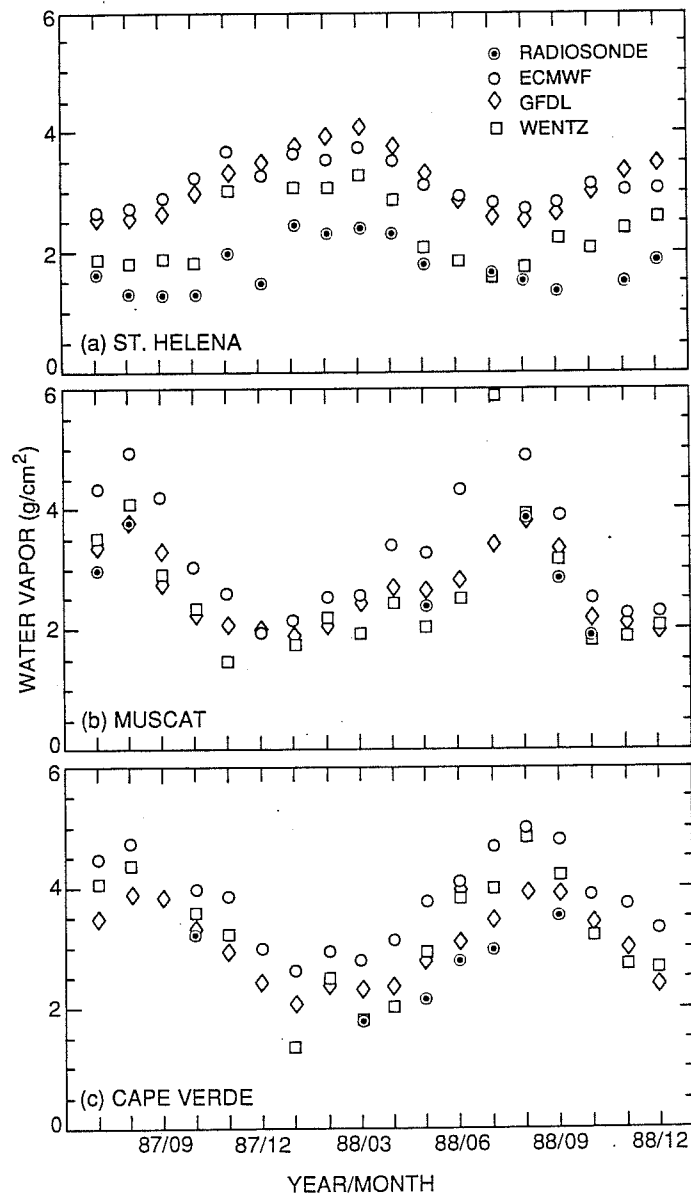


Fig.9. Comparison of the monthly integrated water vapor in the atmospheric column as measured by radiosondes, by spaceborne microwave radiometer (WENTZ), derive from climatology of the Geophysical Fluid Dynamic Laboratory, and produced by the general circulation model of the European Center for Medium Range Weather Forecast.

## 5. CONCLUSION

Bulk parameterization is the practical way to estimate large-scale and long-period ocean-atmosphere water vapor and latent heat exchanges. In smooth flow, recent experimental results confirmed the postulation by Liu et al. (1979) that  $C_E$  increases sharply with decreasing wind. At low winds, conventional constant  $C_E$  underestimates the evaporation. At high winds, recent preliminary experimental results affirmed that  $C_E$  does not increase with  $U$ , as  $C_D$ . Evaporation over ocean at 100 km and 10 day resolutions can be derived from operational satellite data to useful accuracy. Latent heat flux derived from SMMR observations have helped to understand the annual and interannual variabilities of the hydrologic balance in the tropical Pacific and the ocean's response to surface thermal forcing. AGCMs have provided surface evaporation by assimilating measurements. However, large systematic error due to overestimation of atmospheric moisture are found, particularly the data-sparse and dry regions over the southern oceans. The discrepancy may be a result of errors in operational infrared sounder data assimilated into the model. The error may also be caused by interpolation of very sparse *in situ* data in areas of sharp gradients. Improvement in the hydrologic parameterization in AGCM is needed and methods in assimilation SSMI moisture information in AGCM should be developed.

## ACKNOWLEDGMENTS

This study was performed at the Jet Propulsion Laboratory, California Institute of Technology, under contract with the National Aeronautics and Space Administration (NASA). It was supported, in part, by the Earth Observation Program of NASA. Wenqing Tang provided computer programming support.

## REFERENCES

- Alishouse, J.C., S. Snyder, and R.R. Ferraro, 1990: Determination of oceanic total precipitable water from the SSM/I, *IEEE Trans. Geosci. and Remote Sensing*, 28, 811-822.
- Bradley, E.F., P.A. Coppin, and J.S. Godfrey, 1990: Air-sea heat exchange in the western equatorial Pacific ocean I. Sensible and latent heat fluxes. *J. Geophys. Res.*, submitted.
- Bunker, A.F., 1976: Computation of surface energy flux and annual air-sea interaction cycles of the North Atlantic Ocean. *Mon. Wea. Rev.*, 104, 1122-1140.
- Busch, N.E., 1977: Fluxes in the surface boundary layer over the sea. *Modeling and Prediction of the upper layers of the Oceans*, E.B. Kraus (Ed.), Pergamon Press, 72-91.
- Businger, J.A., 1973: A note on free convection. *Boundary Layer Meteor.*, 4, 323-326.
- Charnock, H., 1955: Wind stress on a water surface. *Quart. J. Roy. Meteor. Soc.*, 81, 639-640.
- Deissler, R.G., and C.S. Eian, 1952: Analytical and experimental investigation of fully developed turbulent flow of air in a smooth tube with heat transfer with variable fluid properties. *NACA Tech. Note* 2629.
- Edson, J.B., C.W. Fairall, S.E. Larsen, and P.G. Mestayer, 1988: Progress report from the inertial dissipation group. *Proc. Humidity Exchange Over the Sea Main Experiment (HEXMAX) Analysis and Interpretation*, W.A. Oost, S.D. Smith, K.B. Katsaros (eds.), University of Washington, Seattle, 44-57.
- Friehe, C. A., and K. F. Schmitt, 1976: Parameterization of air-sea interface fluxes of sensible heat and moisture by the bulk aerodynamic formulas. *J. Phys. Oceanogr.*, 12, 801-809.

- Golitsyn, G.S., and A.A. Grachov, 1986: Free convection of multi-component media and parameterization of air-sea interaction at light winds. *Ocean-Air Interactions*, 1, 57-78.
- Hsu, S.A., and B.W. Blanchard, 1989: The relationship between total precipitable water and surface-level humidity over the sea surface: a further evaluation. *J. Geophys. Res.*, 94, 14539-14545.
- Katsaros, K.B., W.T. Liu, J.A. Businger, and J.E. Tillman, 1977: Heat transport and thermal structure in the interfacial boundary layer measured in an open tank of water in turbulent free convection. *J. Fluid Mech.*, 83, 311-335.
- Kondo, J., Y. Fujinawa, and G. Naito, 1973: High frequency component of ocean waves and their relation to aerodynamic roughness. *J. Phys. Oceanogr.*, 3, 197-202.
- Krishnamurti, R., 1973: Further studies on transition to turbulent convection. *J. Fluid Mech.*, 60, 285-303.
- Large, W.G., and S. Pond, 1982: Sensible and latent heat flux measurements over the ocean. *J. Phys. Oceanogr.*, 12, 464-482.
- Liu, W.T., 1974: *Thermal Structure and Heat Transport in the Molecular Boundary Layer under an Evaporating Surface of a Deep Tank of Water*. Master Thesis, University of Washington.
- Liu, W.T., 1986: Statistical relation between monthly precipitable water and surface-level humidity over global oceans. *Mon. Wea. Rev.*, 114, 1591-1602.
- Liu, W. T., 1988: Moisture and latent heat flux variabilities in the tropical Pacific derived from satellite data. *J. Geophys. Res.*, 93, 6749-6760, 6965-6968.
- Liu, W.T., and C. Gautier, 1990: Thermal forcing on the tropical Pacific from satellite data. *J. Geophys. Res.*, 95, 13209-13217.
- Liu, W.T., K.B. Katsaros, and J.A. Businger, 1979: Bulk parameterization of air-sea exchanges of heat and water vapor including the molecular constraints at the surface. *J. Atmos. Sci.*, 36, 1722-1735.
- Liu, W.T., W. Tang, and P.P. Niiler, 1991: Humidity profiles over ocean. *J. Climate*, submitted.
- Nikuradse, J., 1933: Stromungsgesetze in Raubven Rohren. *V.D.I. Forschungsheft* 361.
- Nicholls, S. and C. J. Readins, 1979: Aircraft observations of the structure of the lower boundary layer over the sea. *Quart. J. Roy. Met. Soc.*, 105, 785-802.
- Oort, A.H., 1983: *Global Atmospheric Circulation Statistics*. NOAA Prof. Pap. 14, Natl. Oceanic and Atmos. Admin., Rockville, Md.
- Palmer, T.N., C. Brankovic, and P. Viterbo, 1990: Seasonal simulations of the summer monsoons by the ECMWF model with prescribed SST. *Proc. Intern. TOGA Scientific Conf.*, World Climate Research Programme, Geneva, in press.
- Paulson, C.A., E. Leavitt, and R.G. Fleagle, 1972: Air-sea transfer of momentum, heat and water determined from profile measurements during BOMEX, *J. Phys. Oceanogr.*, 2, 487-497.
- Pond, S., G.T. Phelps, J.E. Paquin, G. McBean, and R.W. Steward, 1971: Measurements of the turbulent fluxes of momentum, moisture and sensible heat over the ocean. *J. Atmos. Sci.*, 28, 901-917.

Reichardt, H., 1940: Die Wärmeübertragung in turbulenten Reibungsschichten *Z. Angew. Math. Mech.*, 20, 297-328.

Schlichting, H., 1968: *Boundary Layer Theory*, McGraw Hill, New York.

Schumann, U., 1988: Minimum friction velocity and heat transfer in the rough surface layer of a convective boundary layer. *Bound. Layer Meteor.*, 44, 311-326.

Schlüssel, P., and W. Emery, 1990: Atmospheric water vapour over oceans from SSM/I measurements. *Int. J. Remote Sensing*, 11, 753-766.

Simonot, J.Y., and H. Le Treut, 1987: Surface heat fluxes from a numerical weather prediction system. *Clim. Dyn.*, 2, 11-28.

Smith, S.D., and R.J. Anderson, 1988: Bedford Institute of Oceanography eddy flux measurement during HEXMAX, *Proc. Humidity Exchange over the Sea Main Experiment (HEXMAX) Analysis and Interpretation*, W.A. Oost, S.D. Smith, and K.B. Katsaros (eds.), University of Washington, Seattle, 14-21.

Wentz, F.J., 1983: A model function for ocean microwave brightness temperatures. *J. Geophys. Res.*, 88, 1892-1908.

Wyngaard, J.C., Cote, O.R., and Izumi, Y., 1971: Local free convection, similarity and budgets of shear stress and heat flux. *J. Atmos. Sci.*, 28, 1171-1182.